Aerodynamics of low-rise buildings subjected to downburst wind loads

Alvaro Mejia [a], Amal Elawady [b],
Arindam Gan Chowdhury [c], Peter Irwin [d], Franklin T. Lombardo [e]

[a] *The Department of Civil and Environmental Engineering, Florida International University, Miami, Florida, USA, ameji023@fiu.edu*
[b] *The Department of Civil and Environmental Engineering, Florida International University, Miami, Florida, USA, aelawady@fiu.edu*
[c] *The Department of Civil and Environmental Engineering, Florida International University, Miami, Florida, USA, chowdhur@fiu.edu*
[d] *The Department of Civil and Environmental Engineering, Florida International University, Miami, Florida, USA, peairwin@fiu.edu*
[e] *University of Illinois at Urbana-Champaign, Urbana, IL, USA, lombaf@illinois.edu*

ABSTRACT

Downbursts are non-stationary, transient, localized wind events that constitute considerable damage to low-rise buildings. The temporal and spatial localization of downburst events and the existence of a travelling main rolling vortex produces outflows with high velocities near the ground leading to wind flow characteristics that significantly differ from Atmospheric Boundary Layer (ABL) winds. This results in different low-rise building aerodynamics. At a newly constructed large-scale downburst simulator at the NSF-NHERI Wall of Wind (WOW), four different rigid models (scaled at 1:100, 1:50, 1:20 and 1:10) representing the Wind Engineering Research Field Laboratory (WERFL) instrumented building at Texas Tech University (TTU) consisting of a one-story, low slope, gabled-roof were tested. The instantaneous pressure coefficients were compared to the field data obtained for an oblique angle of incidence to the full-scale building.

KEYWORDS: Downburst; Low-rise buildings; Pressure Coefficient; Turbulence

1 INTRODUCTION

Most structures built all over the world can be categorized as low-rise buildings which are used for commercial, industrial, residential and other purposes. These buildings are highly vulnerable to wind damage during hurricanes and extreme wind events such as tornadoes and downbursts. Recent reports (Hoogewind et al., 2017; NOAA, 2018; Dunsavage, 2020) have provided direct evidence of the yearly increase of strong convective thunderstorms accounting for billions of dollars in infrastructure damage and fatalities. To fully understand the detrimental windstorm effects on low-rise buildings, particularly from downbursts, it is essential to simulate their actions on buildings by computational or experimental methods. Few attempts to study the effects of downbursts affecting low-rise buildings were conducted which limits the crucial understanding of the wind-structure interaction occurring at the building walls and roof such as the formation of conical vortices, vortices on the rear face of the building, flow separation and vortex shedding. One of the first studies utilized large eddy simulations to assess the unsteady, turbulent flow field of a downburst hitting a small-scale low-rise cubic building by Nicholls et al., 1993. The study presented a series of flow streamlines passing round the cubic building and showed the separation region at the windward corner. A rotating eddy was observed forming behind the building. Lombardo and Smith, 2009a, 2009b; Lombardo et al., 2018 reported aerodynamic loads on the Texas Tech University (TTU) WERFL building from real downburst that occurred on June 19th, 2003, at Lubbock Texas . The TTU WERFL building is a 9.14 m wide by 13.72 m long by 3.96 m high, gable, low-rise building with a roof slope of 1.27° instrumented with pressure taps. From their studies, instantaneous peak pressure coefficients $C_{p,3\sec,Inst}$ were noted to experience a rapid increase in suction (negative) values which exceeded those design GC_p values presented in the ASCE 7-05 standard. Experimentally, Impinging Jet (IJ) methods have been the most popular methods for testing the aerodynamics of low-rise buildings and these consist of a steady IJ in a static position (Chay and Letchford, 2002; Chen, 2011; Zhang et al., 2013, 2014a, 2014b; Li and Ou, 2014; Jubayer et al., 2016), Pulsed IJ also in a static position (Mason et al., 2009; Iida et al., 2015; Jesson et al., 2015a, 2015b), Steady IJ with a translational motion at a specified velocity (Letchford and Chay, 2002; Sengupta and Sarkar, 2008) and a pulsed IJ also with translational motion (Hoshino et al., 2018; Asano et al., 2019). The purpose of this paper is to assess the aerodynamics of a low-rise building using different scaled models tested in a large-scale downburst simulator at the National Science Foundation (NSF) Natural Hazard Engineering Research Infrastructure (NHERI) Wall of Wind (WOW) Experimental Facility (EF). More details about the WOW EF downburst simulator is provided in the next section. The experimental results are compared to field data recorded for the TTU WERFL building during the downburst event that occurred on June 19th, 2003, at Lubbock Texas.

2 METHODOLOGY

Four different rigid models representing the Texas Tech University (TTU WERFL) experimental building of various length scales of 1:00, 1:50, 1:20 and to 1:10 have been subjected to downburst-like outflows in the newly constructed large-scale downburst simulator at the NHERI WOW EF as seen in Figure 1. The downburst simulator adopts the 2D wall jet technique and is placed directly in front of the existing WOW flow management box outlet. The WOW EF is a large-scale, open jet wind testing facility capable of simulating maximum horizontal wind speeds up to 72 m/s. More information about the WOW EF can be found in Chowdhury et al., 2017. For the downburst simulator, the lower region consists of two louver-slats, covering an opening of 1.52 m high by 5.94 m wide cross-section and upper region completely covered by a blockage wall. The louver slats are always positioned vertically to remain closed and will suddenly open to a specified angle from the vertical plane with the assistance of a pulley system and release of counterweights. The scale building models are instrumented with pressure taps of 2 mm diameter with flexible tubing of adequate length. The tubing were connected to a Scanivalve ZOC33/64Px electronic pressure scanner. The pressure measurements were conducted using a digital service module DSM 4000 as the data acquisition system (DAS). The sampling rate used was 520 Hz. The total number of pressure taps used were 204 and the positioning of the pressure taps for each of the scale building model is identical to the pressure tap configuration presented in Lombardo et al., 2018 and seen in Figure 2. Eight incidence wind angles of downburst testing on the scale model buildings (0°, 45°, 90°, 135°, 180°, 225°, 270° and 315°) were considered for all models except for the TTU 1:10 scale building model in which only the 45° wind angle of incidence was obtained. Figure 3 shows all the scaled building models tested.

Figure 1 Downburst simulator at WOW with the two louver slats opened at 45°

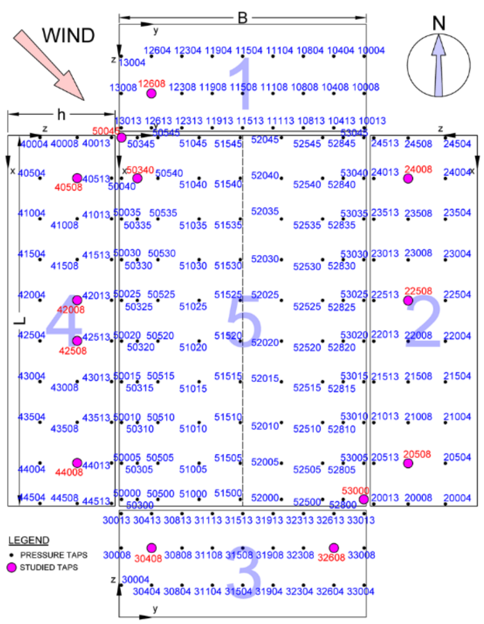

Figure 2 TTU WERFL Building sides and pressure tap ID number configuration with strategically studied pressure taps

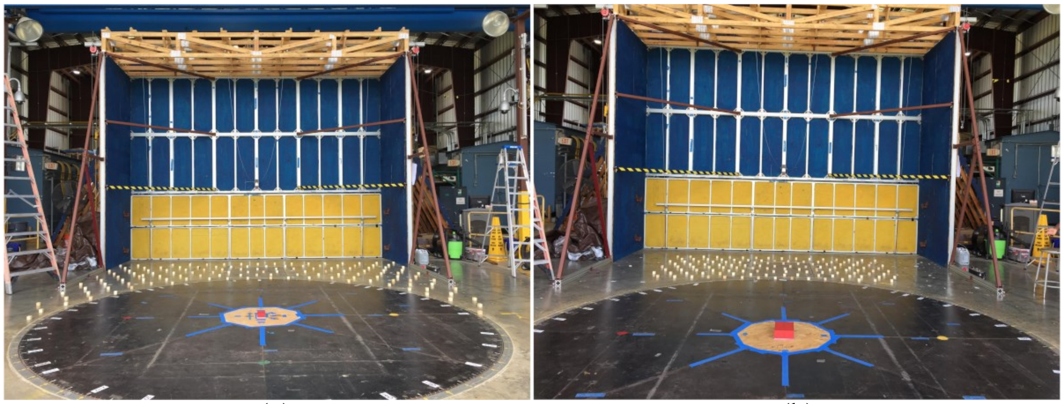

(a) (b)

(c) (d)

Figure 3 Downburst aerodynamic testing on four TTU scale building models: (a) 1:100 in open terrain (b) 1:50 in open terrain (c) 1:20 in terrain with $z_0 = 0.005$ m (d) 1:10 in smooth terrain

The downburst tests were conducted with a slat opening at 45° with respect the vertical plane. The slats were then closed after 10 seconds. The analysis procedure in this paper is divided in two parts. The first part evaluates the statistical and turbulence characteristics of the oncoming downburst outflow. The common analysis for non-synoptic wind phenomena such as downbursts consists in decomposing the wind velocity time history using a moving time average filter, T_{ave} into the sum of the slowly-varying mean $\bar{U}$ plus a residual fluctuation u'. The residual fluctuation u' can then be reduced if it is divided by the standard deviation of the same residual fluctuations $\sigma_{u'}$ providing a new reduced dimensionless fluctuation $\widetilde{u'}$ so that the nonstationary event can be now analyzed as a stationary and Gaussian process (as in the case of ABL), with zero mean and unit standard deviation (Solari et al., 2015). The second part evaluates the instantaneous external surface pressure coefficients and distribution in comparison to a full-scale downburst event impact on the TTU WERFL building.

3 RESULTS

3.1 *Flow characterization*

The three main characteristics of a downburst outflow are the formation of a main rolling vortex in an outflow region, the vertical profile of horizontal wind velocities resembling a 'nose shape' and the transient peak zone (spike) found in the velocity time history profile. The following Figure 4 shows the main rolling vortex in an open terrain condition from a downburst test at the WOW EF. The 2-D wall jet exits a slot as the two louver slats abruptly rotate open to a 45° angle and form a single main rolling vortex that travels through the testing section and grows in size.

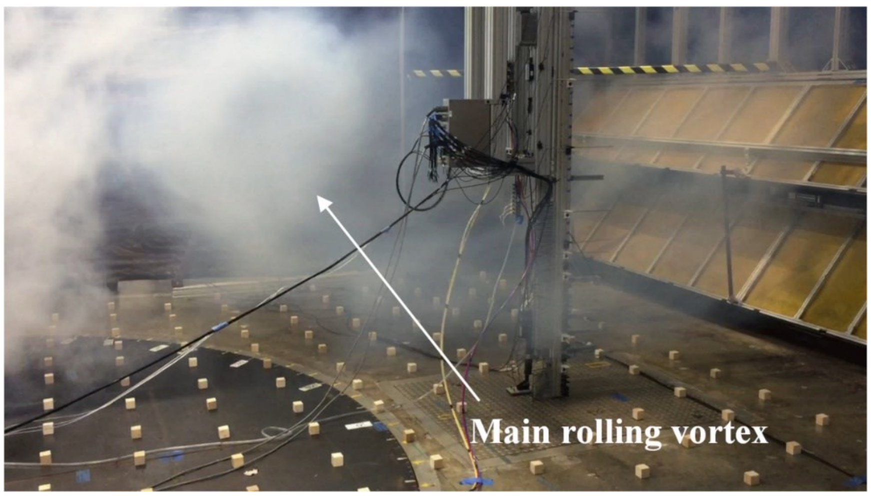

Figure 4 Formation of the downburst characteristic main rolling vortex with the louver slats opened at 45°

In this paper, only the results obtained for the 1:20 model scale will be presented. The velocity time history at the eave height of the TTU 1:20 building ($z = 198.12$ mm) is measured and filtered with an equivalent 3-sec time average obtained from the following equation (1) presented below:

$$T_{ave,m} = \frac{U_{p,\max}}{U_{m,\max}} \cdot \frac{z_m}{z_p} \cdot T_{ave,p} \quad (1)$$

Where $T_{ave,m}$ and $T_{ave,p}$ is the model and prototype selected time average, $U_{m,\max}$ and $U_{p,\max}$ is the maximum instantaneous velocity of the model and prototype, z_m and z_p is the building eave height of the model and prototype respectively. The 3-sec gust is the time average $T_{ave,p}$ used in filtering the full-scale velocity time history. The 3-sec equivalent time averaged $T_{ave,m}$ for the velocity time histories measured at the eave of the 1:20 scaled model were calculated and corresponded to 0.313 sec. Figure 5 shows the velocity time histories comparison for the TTU 1:20 in a terrain with a $z_0 = 0.005$ m and the full-scale TTU.

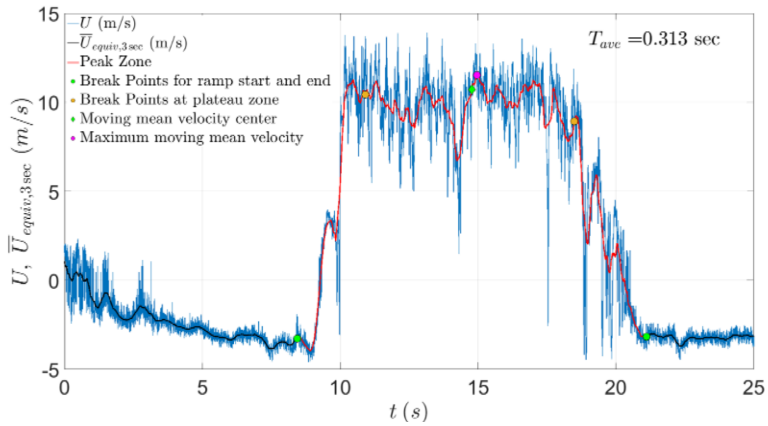

(a)

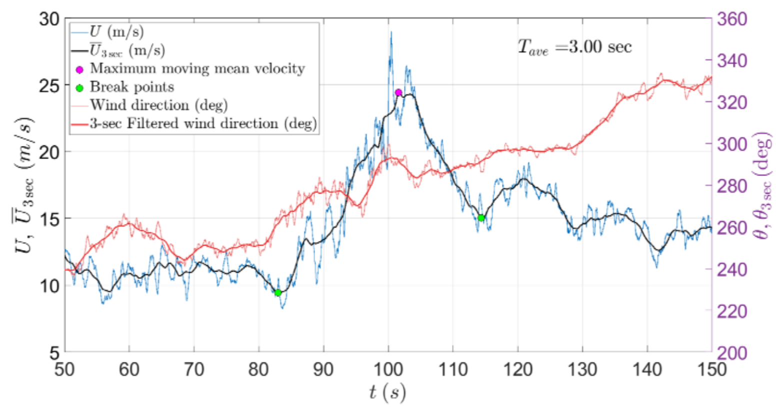

(b)

Figure 5 (a) Velocity time history of the instantaneous and filtered velocity $\overline{U}_{equivalent,3\text{sec}}$ at the eave height of the TTU 1:20 scaled building in a terrain with a $z_0 = 0.005$ m (b) Velocity time and direction history of the instantaneous and filtered velocity $\overline{U}_{3\text{sec}}$ and direction $\bar{\theta}_{3\text{sec}}$ at the eave height of the TTU full-scale building in open terrain (measured at 4 m height of the 50 m high anemometer tower at an approximately 50 meters NW from the building)

The Power Spectral Density (PSD) for the reduced turbulence $\widetilde{u'}$ (Solari et al., 2015; Le and Caracoglia, 2019) of the flow at the 1:20 scale building model height is presented in Figure 6.

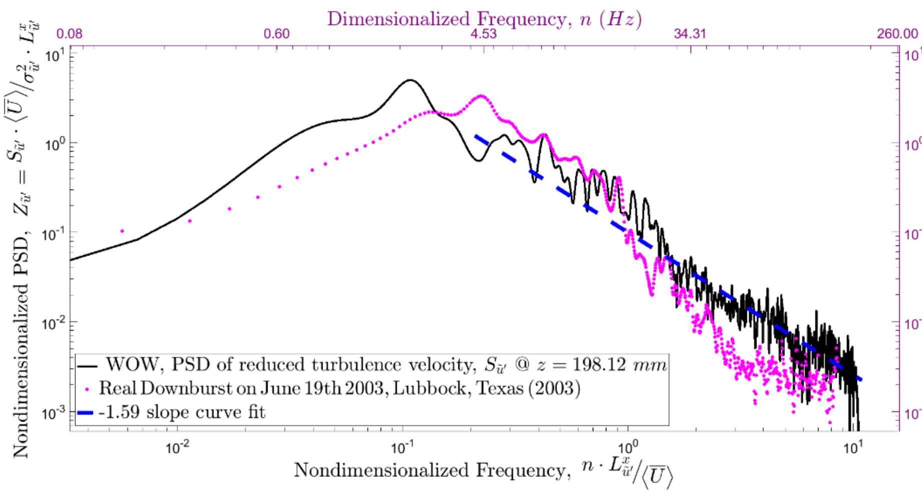

Figure 6 PSD of the reduced fluctuations $\widetilde{u}'$ of the downburst passing at the eave height of TTU 1:20 scale building model and 4 m eave height of the full-scale TTU building measured at the anemometer tower

The PSD of reduced turbulence $\widetilde{u}'$ results show a relatively good agreement on the high frequency end with a slope close to -5/3 (-1.67) between the TTU 1:20 scaled experiment and full-scale. A small gap was seen on the low frequency side when comparing it to the PSD of reduced turbulence $\widetilde{u}'$ of the real downburst that occurred in Lubbock Texas, in June 19th 2003 and impacted the full-scale TTU building. The full-scale downburst was measured at a 4 m height in the 50 m high anemometer tower located at approximately 50 m NW from the TTU building (Lombardo and Smith, 2009b; Lombardo et al., 2018).

3.2 *Comparison to full-scale downburst aerodynamic measurements*

In this section, a comparison between the field measurements obtained by Lombardo et al., 2018 and the experimental values tested at the WOW EF for pressure data on the TTU building is conducted. The procedure implemented by Lombardo et al., 2018 was to obtain the instantaneous observed 3-sec value of the pressure coefficient distribution at all building sides at the time of maximum suction pressure in the upper left corner tap of the building roof (Northwest corner). The following Equations (2) and (3) describe this relationship as follows:

$$\widehat{U}_{3\mathrm{sec}} = \max(\overline{U}_{3\mathrm{sec}}) \tag{2}$$

$$C_{p.3\mathrm{sec},inst.} = \frac{p(t_{peak}) - p_{atmospheric}}{{}^{1}\!/_{2} \cdot \rho_{air} \cdot \widehat{U}^2_{3\mathrm{sec}}} \tag{3}$$

where p is the observed pressure value, $p_{atmospheric}$ is the standard atmospheric pressure, ρ_{air} is the air density, t_{peak} is the time of the maximum suction pressure of an observed 900 sec pressure coefficient time history recorded at the northwest corner tap (Tap ID#50045) which corresponds to 105 sec as represented in Lombardo et al., 2018. In the study here, a similar procedure was followed by obtaining the t_{peak} to be at the time at which the equivalent 3-sec filtered pressure coefficient $C_{p,equiv,3\text{sec}}$ (using a corresponding $T_{ave,m} = 0.313$ sec) of the same northwest corner tap (Tap ID#50045) reaches the maximum suction value. $\widehat{U}_{3\text{sec}}$ is the maximum horizontal 3-sec moving mean wind velocity in the downburst outflow at the corresponding building eave height but independent of t_{peak} as it bears no relevance to the structural designer if the times of maximum suction pressure or maximum moving mean velocity do not coincide. The following Figures 7(a) and 7(b) show the 3-sec filtered pressure coefficient time histories of the TTU 1:20 and the full-scale 3-sec filtered pressure coefficients $C_{p,3\text{sec}}$ of the observed 900 sec time histories.

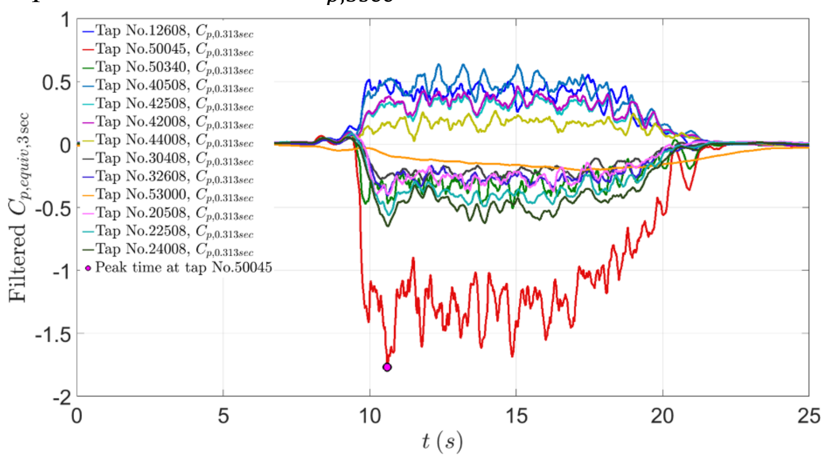

(a)

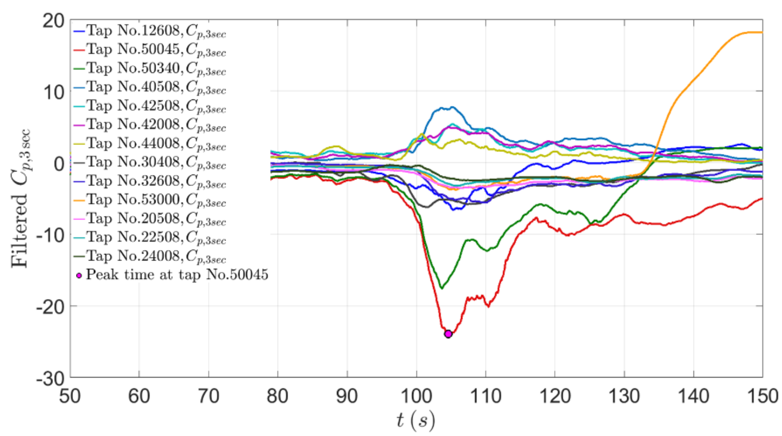

(b)

Figure 7 (a) Filtered 3-sec equivalent pressure coefficient time history ($C_{p,equiv,3\text{sec}}$) of the studied pressure taps at the TTU 1:20 scaled building in a terrain with a $z_0 = 0.005$ m (b) Filtered 3-sec pressure coefficient time history ($C_{p,3\text{sec}}$) of the studied pressure taps at the TTU full-scale building in open terrain. The peak times for northwest corner tap ID#50045 are shown.

Figure 8(a) and (b) show the observed peak pressures obtained from the full-scale measurement at an instantaneous wind direction of 218° and the TTU 1:20 scale experiment results at a constant wind direction of 315° in a terrain with surface roughness of $z_0 = 0.005$ m, respectively . It can be seen from Figure 8(a) and (b) that the upstream flow separates at the leading edge of the roof creating a separation bubble on both cases. The separation bubble is a turbulent recirculating flow region that is responsible for causing large-magnitude suction pressures (uplift) on the roof surface. At oblique angles of incidence of 315° as shown in Figure 8**Error! Reference source not found.**(b), larger suction regions are observed on the experimental TTU 1:20 roof when compared to the full-scale roof. For the full-scale case, conical vortices were not pronounced. This could be because the angle of attack (AOA) at the particular peak time is different from the "mean" AOA. Also, another reason could be the fact that the measurement tower was 50 m away which may cause less accurate measurement of AOA at the building location. The magnitudes of negative and positive pressures of the full-scale and the TTU 1:20 model test, despite the difference in angle of incidence, were as follows. A peak suction value of $\widehat{C}_{p,3sec,inst}$=-5.42 was obtained in the upper left corner of the roof in the full-scale TTU exceeding a $\widehat{C}_{p,3sec,inst}$=-3.28 in the TTU 1:20 experiment. For side walls experiencing suction pressures (sidewall #2 and sidewall #3), the TTU 1:20 peak suction pressures slightly exceeded those found in the full-scale TTU building measurements. The peak positive pressures in sidewall #4 of the full-scale TTU exceeded those in the TTU 1:20 model but not in the north wall.

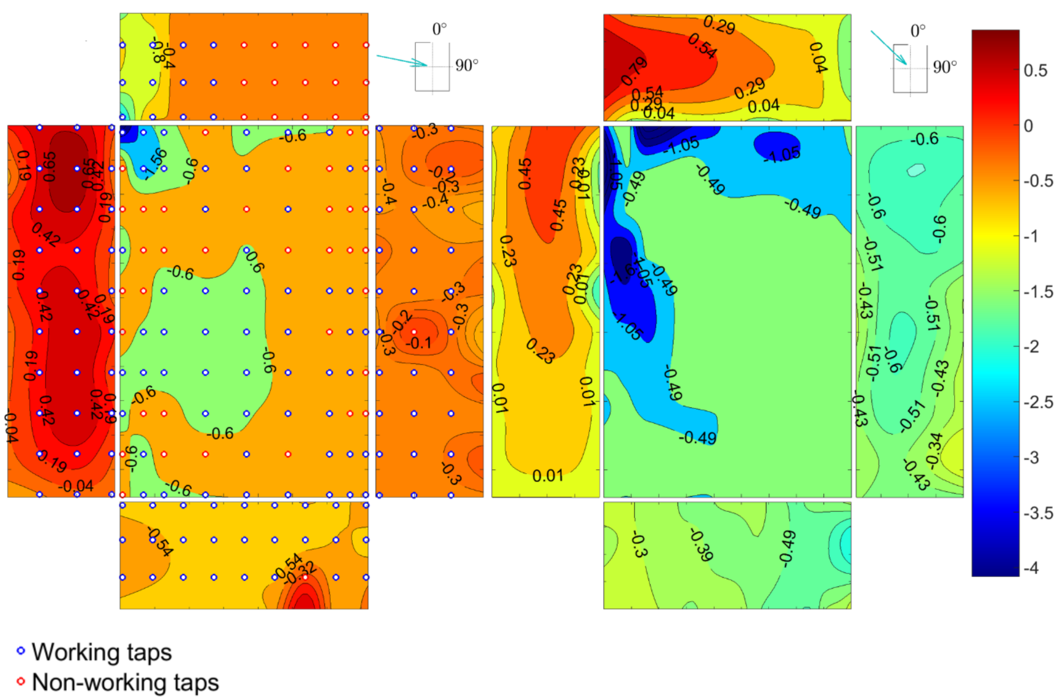

(a) (b)

Figure 8 Instantaneous observed pressure coefficient $C_{p.3sec,Inst}$ for the: (a) Full-scale TTU building with a Downburst instantaneous wind angle of incidence of 282°; (b) TTU 1:20 in a smoother terrain with $z_0 = 0.005$ m and downburst at 315°.

4 CONCLUDING REMARKS

The simulation of a large-scale downburst is of great importance for the wind and structural engineering community as it minimizes detrimental scale-effects found in small-scale testing and creates a new reliable aerodynamic database for downburst testing. A relatively large-scale downburst aerodynamic study was conducted on the TTU WERFL building models at the NHERI WOW EF. The satisfactory results in the downburst outflow meet the three main characteristics: main rolling vortex, spike in the velocity time history and vertical 'nose' profile in the horizontal wind velocities as found at the WOW downburst experiments. Comparisons to the field measurements of the same building's aerodynamics under a real downburst event are reported. A statistical turbulence characterization was evaluated on the oncoming outflow using the PSD analysis on the reduced turbulence $\widetilde{u'}$ velocities from this large-scale downburst simulator at WOW. The results showed a good agreement on the high and low frequency ends when compared to scaled-down and full-scale downburst prior measurements.

The downburst aerodynamic behavior of the TTU WERFL building showed noticeable differences between the full-scale TTU and the model TTU 1:20 in the pressure distribution of instantaneous $C_{p.3\text{sec},inst.}$ at the peak time of the upper left corner tap located in the roof. These differences could be due to the difficulties encountered in the field that are not found in a controlled experimental environment. For example, the variation of the angle of incidence during the passage of the downburst round the building affected the formation of the conical vortices not being noticeable in the full-scale experiments. Such a varying wind direction was not simulated in the laboratory. A good agreement between the observed peak positive and negative pressures. More studies are encouraged in this research area to achieve an understanding of downburst impacts on low-rise buildings.

ACKNOWLEDGEMENTS

All experiments were conducted at the US-NSF (CMMI #1520853 and No. 2037899) NHERI Wall of Wind Experimental Facility. The Authors wish to thank the NHERI WOW EF personnel for conducting the downburst tests satisfactorily. The authors sincerely acknowledge the financial contribution of The State of Florida Division of Emergency Management (FLDEM). The opinions of the authors expressed herein do not necessarily state or reflect those of the sponsors.

REFERENCES

Asano, K., Iida, Y., Uematsu, Y., 2019. Laboratory study of wind loads on a low-rise building in a downburst using a moving pulsed jet simulator and their comparison with other types of simulators. J. Wind Eng. Ind. Aerodyn. 184, 313–320.

ASCE 7-05, 2005. Minimum Design Loads for Buildings and Other Structures: ASCE/SEI

Standard 7-05.

Chay, M.T., Letchford, C.W., 2002. Pressure distributions on a cube in a simulated thunderstorm downburst—Part A: stationary downburst observations. J. Wind Eng. Ind. Aerodyn. 90, 711–732.

Chen, Y., 2011. Experimental investigation of spherical roof subjected to thunderstorm downbursts. Jianzhu Jiegou Xuebao(Journal Build. Struct. 32, 26–33.

Chowdhury, A., Zisis, I., Irwin, P., et al., 2017. Large-scale experimentation using the 12-fan wall of wind to assess and mitigate hurricane wind and rain impacts on buildings and infrastructure systems. J. Struct. Eng. 143, 4017053.

Dunsavage, J., 2020. Evolving risks call for innovation to reduce costs, drive resilience 1–15.

Hoogewind, K.A., Baldwin, M.E., Trapp, R.J., 2017. The impact of climate change on hazardous convective weather in the United States: Insight from high-resolution dynamical downscaling. J. Clim. 30, 10081–10100.

Hoshino, N., Iida, Y., Uematsu, Y., 2018. Effects of non-stationarity of downburst on the wind loading of buildings. J. Wind Eng. 43, 1–13.

Iida, Y., Uematsu, Y., Gavanski, E., 2015. A study of downburst-induced wind loading on buildings. J. Wind Eng. 40, 40–49.

Jesson, M., Sterling, M., Letchford, C., Baker, C., 2015a. Aerodynamic forces on the roofs of low-, mid-and high-rise buildings subject to transient winds. J. Wind Eng. Ind. Aerodyn. 143, 42–49.

Jesson, M., Sterling, M., Letchford, C., Haines, M., 2015b. Aerodynamic forces on generic buildings subject to transient, downburst-type winds. J. Wind Eng. Ind. Aerodyn. 137, 58–68.

Jubayer, C., Elatar, A., Hangan, H., 2016. Pressure distributions on a low-rise building in a laboratory simulated downburst, in: Proceedings of the 8th International Colloquium on Bluff Body Aerodynamics and Applications, Boston, Massachusetts, USA.

Le, V., Caracoglia, L., 2019. Generation and characterization of a non-stationary flow field in a small-scale wind tunnel using a multi-blade flow device. J. Wind Eng. Ind. Aerodyn. 186, 1–16.

Letchford, C.W., Chay, M.T., 2002. Pressure distributions on a cube in a simulated thunderstorm downburst. Part B: moving downburst observations. J. Wind Eng. Ind. Aerodyn. 90, 733–753.

Li, H., Ou, J., 2014. Pressure distributions on prism-shaped buildings in experimentally simulated downburst. Sci. China Technol. Sci. 57, 2070–2081.

Lombardo, F.T., Mason, M.S., de Alba, A.Z., 2018. Investigation of a downburst loading event on a full-scale low-rise building. J. Wind Eng. Ind. Aerodyn. 182, 272–285.

Lombardo, F.T., Smith, D., 2009a. Analysis and interpretation of thunderstorm wind flow and its effects on a bluff body.

Lombardo, F.T., Smith, D.A., 2009b. Analysis and interpretation of non-stationary wind flow on a bluff body, in: 11th Americas Conference on Wind Engineering.

Mason, M.S., James, D.L., Letchford, C.W., 2009. Wind pressure measurements on a cube subjected to pulsed impinging jet flow. Wind Struct. 12, 77–88.

Nicholls, M., Pielke, R., Meroney, R., 1993. Large eddy simulation of microburst winds flowing around a building, in: Computational Wind Engineering 1. Elsevier, pp. 229–237.

NOAA, 2018. National Oceanic and Atmospheric Administration, Office for Coastal Management [WWW Document]. URL https://www.noaa.gov/

Sengupta, A., Sarkar, P.P., 2008. Experimental measurement and numerical simulation of an impinging jet with application to thunderstorm microburst winds. J. Wind Eng. Ind. Aerodyn. 96, 345–365.

Solari, G., Burlando, M., De Gaetano, P., Repetto, M.P., 2015. Characteristics of thunderstorms relevant to the wind loading of structures. Wind Struct. 20, 763–791.

Zhang, Y., Hu, H., Sarkar, P.P., 2014a. Comparison of microburst-wind loads on low-rise structures of various geometric shapes. J. Wind Eng. Ind. Aerodyn. 133, 181–190.

Zhang, Y., Hu, H., Sarkar, P.P., 2013. Modeling of microburst outflows using impinging jet and cooling source approaches and their comparison. Eng. Struct. 56, 779–793.

Zhang, Y., Sarkar, P., Hu, H., 2014b. An experimental study on wind loads acting on a high-rise building model induced by microburst-like winds. J. Fluids Struct. 50, 547–564.